Multiple scattering of slow ions in a free-electron gas

Claudio D. Archubi and Néstor R. Arista

División Colisiones Atómicas, Instituto Balseiro and Centro, Atómico Bariloche, RA-8400 Bariloche, Argentina

We study the influence of electronic scattering on the angular distributions of ions and atoms moving through a free-electron gas. We present a general formulation based on the multiple-scattering formalism, using two alternative descriptions: a linear approach based on Lindhard's dielectric function, and a nonlinear treatment based on density functional calculations. We obtain analytical expressions for the multiple-scattering function and for the half-width of the distribution. We show the results of several calculations for slow hydrogen and helium and their isotopes. We analyze the results and obtain analytical approximations for all of the cases. The magnitude of the electronic effects on the multiple scattering distribution is determined and compared with previous estimations.

I. INTRODUCTION

Multiple scattering is one of the characteristic processes in the interaction of ionized projectiles with matter. As a result of the multiple interactions produced when a beam of particles penetrates a medium, the angular distribution of the incident particles is progressively spread. This process has been extensively studied. The basic theory of this phenomenon was developed by several authors using various statistical approaches [1–8], and applied in numerous studies dealing with the penetration of electrons and ion beams in matter. A complete review of the earlier developments was given in Ref. [6].

One question of basic interest which has not been adequately studied so far is the contribution to the angular dispersion produced by the interaction between the incident ions and the target electrons. This contribution is frequently neglected on the basis of the very small mass ratio between the electrons and the incident ions. However, in special cases, like in the channeling of light ions [9] (including, in particular, muons and pions [10–12]), where the atomic collisions with target atoms is strongly reduced and the angular spread of the beam is significantly narrow, the contribution of scattering processes due to interactions with the valence electrons inside the channel may produce a non-negligible effect on the final channeling results.

To the best of our knowledge, a first estimation of the effects of electronic scattering in the case of swift ions was given by Lindhard [13] who derived a formula that relates the angular spread produced by electronic interactions to the corresponding stopping power, in the form

$$\langle \delta \Phi^2 \rangle_L = \frac{m}{(M_1 v)^2} S_e n_e x, \tag{1}$$

where m is the electron mass, M_1 and v are the mass and velocity of the incident ion, n_e and x are the electron density and thickness of the target, and S_e is the electronic stopping cross section. However, this relation only applies to the case of swift ions due to the condition that the target particle is assumed to be at rest before the collision, a situation that

does not apply to the case of ions with velocities smaller than the Fermi velocity of the target electrons.

A complementary estimation based on Lindhard's arguments, but for slow ions, was given by Bonderup [14] who derived an upper limit to the angular spread $\langle \delta \Phi^2 \rangle$ due to electronic interactions, in the form: $\langle \delta \Phi^2 \rangle < \langle \delta \Phi^2 \rangle_B$ with

$$\langle \delta \Phi^2 \rangle_B = 8 \left(\frac{m v_F}{M_1 v} \right)^2 \sigma_{tr} n_e x, \tag{2}$$

where v_F is the Fermi velocity of the electron gas and σ_{tr} is the transport cross section. Note that this expression may be also related to the stopping power using the low-energy expression [14], $S_e = m v v_F \sigma_{tr}$, in the form

$$\langle \delta \Phi^2 \rangle_B = \frac{8m}{(M_1 v)^2} \frac{v_F}{v} S_e n_e x, \tag{3}$$

an expression that may be readily compared with the high-energy approximation of Eq. (1).

However, as stated by Bonderup [14], it is difficult to assess the degree of the overestimate contained in this expression. Hence, the contribution of electronic processes to the multiple scattering of slow ions is a question that clearly deserves a quantitative study.

Here we provide the theoretical description of the effects of the electronic interactions on the angular spread of the beam for the case of slow ions interacting with a free-electron gas (FEG) representing the valence electrons of a solid. The formulation is based, on the one side, on the standard theory of multiple scattering in random media (which is particularly appropriate for a FEG), and on the other, on two alternative representations of the interaction between slow ions and the electrons in a solid: the linear description provided by the dielectric function formalism [15,16], and the nonlinear representation emerging from previous density functional calculations [17,18].

The basic formulation of the momentum transfer probability in single-scattering theory is described in Sec. II, considering first the linear or dielectric approximation, and then we reformulate the analysis within the framework of nonlinear calculations (density functional theory). In Sec. III we

introduce the previous results in the formalism of the multiple-scattering theory.

In Sec. IV we discuss in a general way the various results and obtain analytical fitting formulas for the value of the half angle of the multiple-scattering distributions, which apply on the wide range of electron densities in solids. The magnitude of the electronic contribution to the multiple-scattering effect is illustrated with examples for some cases of interest. Finally, we compare the present results with Bonderup's estimation. The summary and conclusions are contained in Sec. V.

II. SINGLE SCATTERING

A. Linear approach

We consider first the elementary process of inelastic scattering of an incident ion due to the interaction with the valence electrons of a solid. The electrons will be represented as a free-electron gas with density n_e and Fermi velocity $v_F = 1.919/r_s$ (in atomic units) using the parameter r_s defined as usual by $4\pi r_s^3/3 = 1/n_e$.

Here we first formulate the scattering process following the dielectric function formalism [16,19]. According to Ref. [16], in the dielectric formulation the scattering probability may be expressed as

$$\frac{d^4P}{d^3q\,d\omega} = \frac{|F(q)|^2}{\pi^2 q^2}\,\text{Im}\left[\frac{-1}{\varepsilon(q,\omega)}\right]\delta(\hbar\omega - \hbar\vec{q}\cdot\vec{v}), \quad (4)$$

where $\varepsilon(q,\omega)$ denotes the dielectric function, $\vec{v}$ is the initial ion velocity before the scattering event, and $F(q)$ is the ion form factor defined by

$$F(q) = \int d^3r\,\rho(r)e^{i\mathbf{k}\cdot\mathbf{r}}, \quad (5)$$

where $\rho(r)$ is the ion charge density (assumed as spherically symmetric).

Then, by integrating over the frequency ω we obtain the momentum-loss spectrum

$$\frac{d^3P}{d^3q} = \int \frac{d^4P}{d^3q\,d\omega}d\omega = \frac{|F(q)|^2}{\hbar\pi^2 q^2}\,\text{Im}\left[\frac{-1}{\varepsilon(q,\omega)}\right]_{\omega=\vec{q}\cdot\vec{v}}. \quad (6)$$

We can separate the momentum transfer into parallel ($q_\parallel$) and perpendicular ($q_\perp$) components relative to the initial beam direction, $d^3q = d^2q_\perp\,dq_\parallel$, and by integrating over $q_\parallel$ we get

$$\frac{d^2P}{d^2q_\perp} = \int \frac{d^3P}{d^3q}dq_\parallel$$

$$= \frac{1}{\hbar\pi^2}\int \frac{dq_\parallel}{(q_\parallel^2 + q_\perp^2)}|F(q)|^2\,\text{Im}\left[\frac{-1}{\varepsilon(q,\omega)}\right]_{\omega=q_\parallel\cdot v}. \quad (7)$$

This expression contains the required information on the probability of the differential scattering of the incident ion which produces its angular deflection in single-scattering events, and includes also the collective screening effects produced by the electron gas.

For the evaluation of Eq. (7) we use the low-energy approximation corresponding to ion velocities $v \ll v_F$, v_F being the Fermi velocity of the FEG. Since the available frequencies are restricted by $\omega < qv$, the approximations of interest for the real (ε_1) and imaginary (ε_2) parts of the dielectric function, become [15]

$$\varepsilon_1(q,\omega) \cong \varepsilon_1[q] = 1 + \frac{q_{TF}^2}{q^2} \quad (8)$$

$$\varepsilon_2(q,\omega) \cong \begin{cases} 2K_1\omega/q^3, & q \leq 2k_F \\ 0, & q > 2k_F \end{cases}, \quad (9)$$

where $q_{TF} = \sqrt{3}\,\omega_P/v_F$ and $K_1 = m^2e^2/\hbar^3$.

Using this, we approximate the integral in Eq. (7), assuming $|\varepsilon_2| \ll |\varepsilon_1|$, by

$$\frac{d^2P}{d^2q_\perp} = \frac{1}{\hbar\pi^2}\int \frac{dq_\parallel}{(q_\parallel^2 + q_\perp^2)}|F(q)|^2\left[\frac{\varepsilon_2(q,\omega)}{\varepsilon_1[q]^2}\right]\Bigg|_{\omega=q_\parallel v}, \quad (10)$$

$$= \frac{1}{\hbar\pi^2}\int_0^Q \frac{dq_\parallel}{(q_\parallel^2 + q_\perp^2)}|F(\sqrt{q_\parallel^2 + q_\perp^2})|^2$$

$$\times\left[\frac{2K_1 v q_\parallel\sqrt{q_\parallel^2 + q_\perp^2}}{(q_\parallel^2 + q_\perp^2 + q_{TF}^2)^2}\right]. \quad (11)$$

The value of Q is restricted by the condition stemming from Eq. (9), namely $q = \sqrt{q_\parallel^2 + q_\perp^2} \leq 2k_F$, or: $q_\parallel \leq Q = \sqrt{4k_F^2 - q_\perp^2}$.

Finally, due the azimuthal symmetry we may replace $d^2q_\perp = 2\pi q_\perp\,dq_\perp$ and obtain

$$\frac{dP}{dq_\perp} \equiv v G(r_s, q_\perp) = 4K_1 v\frac{1}{\hbar\pi}q_\perp\int_0^Q \frac{dq_\parallel}{(q_\parallel^2 + q_\perp^2)}|F(\sqrt{q_\parallel^2 + q_\perp^2})|^2$$

$$\times\left[\frac{q_\parallel\sqrt{q_\parallel^2 + q_\perp^2}}{(q_\parallel^2 + q_\perp^2 + q_{TF}^2)^2}\right]. \quad (12)$$

This equation defines the dimensionless function $G(r_s, q_\perp)$, which is independent of the ion velocity v, but depends on the Fermi velocity v_F (or electron gas density n_e) through the parameter r_s. The expression for $G(r_s, q_\perp)$ may be further simplified by expressing the integration in terms of q as follows:

$$G(r_s, q_\perp) = \frac{4m^2e^2}{\hbar^4\pi}q_\perp\int_{q_\perp}^{2k_F} \frac{|F(q)|^2}{(q^2 + \beta^2)^2}dq, \quad (13)$$

where $\beta = q_{TF} = \sqrt{3}\,\omega_P/v_F$ is the FEG screening constant within the linear approximation. In particular, for bare ions, $F(q) = Ze$, this expression has a simple analytical solution,

$$G(r_s, q_\perp) = 2m^2e^2\frac{(Ze)^2}{\hbar^4\pi}\frac{q_\perp}{\beta^2}\left[\frac{q}{q^2 + \beta^2} + \frac{1}{\beta}\arctan\left(\frac{q}{\beta}\right)\right]\Bigg|_{q=q_\perp}^{q=2k_F}. \quad (14)$$

B. Nonlinear approach

As is well known, the linear formulation provides a simplified description of the interaction of slow ions with a free-electron gas, but for quantitative studies, an additional consideration of nonlinear effects must be included [17,18,20–22]. These effects may be described either by introducing higher-order corrections to the scattering amplitude or by reformulating the calculations in a full nonlinear way. The best available representation of the interaction of slow ions with a free-electron gas is the one provided by the density functional approach [18,23]. In this formulation a fixed impurity (either an atom or an ion) is strongly screened by the jellium and the whole system is considered in the ground state. In this case the system is neutralized, which corresponds to the usual picture of hydrogen or helium atoms immersed in a jellium [24,25]. We also note that the usual Density Functional Theory (DFT) calculations actually assume a fixed ion, which is, in fact, appropriate only for the case of very slow ions (there is a more recent extension of the DFT method to the case of moving ions [26] but we will not consider dynamical screening effects in the present analysis).

To introduce the nonlinear approach in the present treatment we will use a direct connection between the scattering amplitudes, in linear and nonlinear descriptions, which was formulated in Ref. [27]. First, we note that Eq. (13) may be written as

$$G(r_s, q_\perp) = \frac{q_\perp}{\pi} \int_{q_\perp}^{2k_F} |f(\theta)|^2 dq, \qquad (15)$$

where

$$f(\theta) = \frac{me}{\hbar^2} \frac{2F(q)}{(q^2 + \beta^2)} \qquad (16)$$

is the scattering amplitude in the linear description of the scattering process (corresponding to the first-order Born approximation), with the usual relation between q and θ: $q = 2k_F \sin(\theta/2)$.

The transition from the linear to the nonlinear formulation can be made by replacing the scattering amplitude by the nonlinear value, which is given by the partial-wave expansion, namely

$$f(\theta) = \frac{1}{k} \sum_l (2l+1) e^{i\delta_l} \sin(\delta_l) P_l(\cos\theta), \qquad (17)$$

where δ_l denotes the phase shift corresponding to the l-wave component and $P_l(x)$ are the Legendre polynomials.

It may be shown that this simple procedure permits us to obtain in a straightforward way all the known expressions for the energy loss moments, including the stopping power [28], the straggling [29], and the total scattering probability (also called "width" of the particle state) [27].

We may further note that if we integrate the present expression for the G function of Eq. (15) over all the possible momentum transfers $(0 < q_\perp < 2k_F)$ we then obtain the correct expression for the total scattering probability per unit time, namely

$$P = v \int_0^{2k_F} G(r_s, q_\perp) dq_\perp = \frac{v}{2\pi} \int_0^{2k_F} |f(\theta)|^2 q^2 dq \qquad (18)$$

which is equivalent to the expression given in Ref. [27].

The present calculations of the multiple-scattering distributions (to be described below) have been made using the expressions of Eqs. (15) and (17) and using the phase shift values calculated for a point charge Ze in an electron gas by Puska and Nieminen [18] with the density functional formulation [30].

III. MULTIPLE SCATTERING

From the previous formulation we obtain an expression for the differential cross section for electron-ion scattering in a FEG, with transverse momentum transfer $\hbar q_\perp$, of the form

$$d\sigma = \frac{1}{n_e v} dP = \frac{1}{n_e} G(r_s, q_\perp) dq_\perp \qquad (19)$$

and we recall also the relation between the momentum transfer $q_\perp$ and the ion angular deflection ψ, in the small-angle approximation, namely $\hbar q_\perp = M_1 v \psi$, as well as the differential relation, $dq_\perp = M_1 v d\psi/\hbar$.

The convolution of the multiple-scattering events, as the particle penetrates a distance x within the solid, is usually represented by the multiple-scattering (MS) function $f(\alpha, x)$ [1–8], which yields the statistical distribution of particles with a total angular deflection α.

Following the formulation of Ref. [8] we express the electronic multiple-scattering (EMS) function [Eq. (1) of Ref. [8]] in the form $F(\alpha, x) d\Omega = f(\alpha, x) d\Omega/2\pi$, where $f(\alpha, x)$ is given in the small-angle approximation by

$$f(\alpha, x) = \int_0^\infty \kappa \, d\kappa \, J_0(\kappa\alpha) \exp[-n_e x \sigma_0(\kappa)]. \qquad (20)$$

The function $\sigma_0(\kappa)$ is determined from the previously defined scattering function $G(r_s, q_\perp)$, for the present case of an electron gas, by

$$\sigma_0(\kappa) = \int [1 - J_0(\kappa\psi)] d\sigma$$

$$= \frac{1}{n_e} \int_0^{2k_F} [1 - J_0(\kappa q_\perp \hbar/M_1 v)] G(r_s, q_\perp) dq_\perp \qquad (21)$$

with $d\sigma$ given by (19) and $\psi = \hbar q_\perp/M_1 v$.

Note that the density factor n_e cancels out in Eqs. (20) and (21), so that we finally obtain the simple expression

$$f(\alpha, x) = \int_0^\infty \kappa \, d\kappa \, J_0(\kappa\alpha) \exp[-x\sigma_0'(\kappa)] \qquad (22)$$

with

$$\sigma_0'(\kappa) = \int_0^{2k_F} [1 - J_0(\kappa q_\perp \hbar/M_1 v)] G(r_s, q_\perp) dq_\perp. \qquad (23)$$

Introducing the variable $\eta = q_\perp/k_F$ in Eq. (23), it may be seen that $\sigma_0'(\kappa)$ becomes a function of the variable ξ

$= \kappa \hbar k_F / M_1 v$ (and depends parametrically on the density through r_s),

$$\sigma_0'(\kappa) = \tilde{\sigma}_0(\xi, r_s) = k_F \int_0^2 [1 - J_0(\xi \eta)] G(r_s, \eta k_F) d\eta.$$

(24)

Then Eq. (22) may be parametrized in terms of $\kappa \alpha = \xi M_1 v \alpha / \hbar k_F$,

$$f(\alpha, x) = \lambda^2 / 2\pi \int_0^\infty \xi \, d\xi \, J_0(\lambda \alpha \xi) \exp[-x \tilde{\sigma}_0(\xi, r_s)] \quad (25)$$

with $\lambda = \kappa / \xi = M_1 v / \hbar k_F$. Hence, the angular dependence of the EMS function $f(\alpha, x)$ is parametrized in terms of $\lambda \alpha = M_1 v \alpha / \hbar k_F$. In particular, this implies that the angular width of the distribution scales like $(M_1 v)^{-1}$. However, we note that a simple scaling with k_F is not obtained due to the additional r_s dependence of the function $G(r_s, q_\perp)$ implicit in Eq. (15).

The scaling with $(M_1 v)^{-1}$ is a new result characteristic of the electronic multiple-scattering process. As is well known, the general scaling of the *atomic* multiple-scattering function corresponding to ion-atom scattering follows $a \sim 1/E$ dependence in the energy range considered here [8,31], being $E = M_1 v^2 / 2$ the incident-ion energy.

IV. RESULTS AND DISCUSSION

We analyze first the distribution of momentum transfers produced by single-collision events, described by the function $G(r_s, q_\perp)$ in Eq. (15).

For slow projectiles, the momentum transfer to the target electrons is restricted by $q < 2k_F$, and the probability function has the characteristics shown in Fig. 1, where we show the functions $G(r_s, q_\perp)$ for hydrogen and helium, obtained with the nonlinear method. It has been shown that these functions are significantly larger than those obtained from the linear formulation for hydrogen and helium atoms (i.e., nonlinear effects produce an enhancement of the scattering intensity as compared with the linear model).

Using the probability function $G(r_s, q_\perp)$ obtained from Eq. (15) we have calculated the distribution function $f(\alpha, x)$ using Eqs. (22) and (23), or, equivalently, (24) and (25).

To analyze the characteristics of the solutions for the EMS function, we introduce the *half-width at half maximum* angle, $\alpha_{1/2}$, for which the distribution function $f(\alpha, x)$ falls to one-half of its maximum value, which corresponds to $\alpha = 0$, namely: $f(\alpha_{1/2}, x) = 0.5 f(0, x)$. This equation is solved numerically to determine the value of $\alpha_{1/2}$ for each of the cases considered in this study. The magnitudes of the angular widths $\alpha_{1/2}$ for hydrogen and helium atoms calculated with the nonlinear approach are significantly larger than those obtained from the linear case. As an example, the numerical results for the EMS function $f(\alpha, x)$ are shown in Fig. 2, where we show the normalized distribution $f(\alpha, x)/f(0, x)$ versus the reduced scattering angle $\alpha / \alpha_{1/2}$. The line in this figure corresponds to a *Gaussian* function having the same angular width, namely $g(\alpha) = \exp(-\Gamma \alpha^2 / \alpha_{1/2}^2)$ with $\Gamma = \ln(2)$. As seen in the figure, the Gaussian approximation yields an
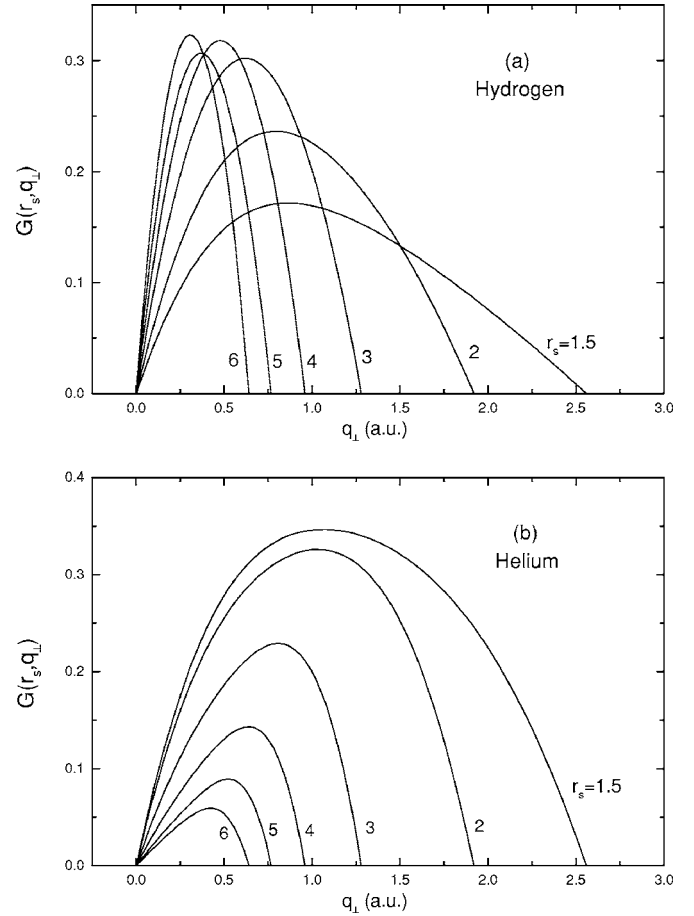

FIG. 1. Probability functions, $G(r_s, q_\perp)$, for the scattering of hydrogen (part *a*) and helium (part *b*) in a free-electron gas with transverse momentum transfer $q_\perp$, according to the nonlinear formulation, for r_s values 1.5, 2, 3, 4, 5, and 6 a.u., as indicated on each curve.

excellent representation of the angular dependence. We have obtained similar Gaussian types of behaviors in almost all of the cases studied, except only in calculations for very thin targets (below ~ 50 Å) where small deviations from the Gaussian shapes were observed in the tails of the distributions, which, however, do not affect the value of the angular width $\alpha_{1/2}$.

The angular width $\alpha_{1/2}$ has been determined for hydrogen, deuterium, muonium, helium, and He_3 for various velocities $v < v_F$ and target thicknesses x (considering always thicknesses much smaller than the corresponding ranges of the particles in the medium for the assumed velocity). The predicted scaling of the angular width $\alpha_{1/2} \sim 1/M_1 v$ with the velocity and the mass of the projectile for a given charge condition (i.e., hydrogen, deuterium, and muonium on one side; helium and He_3 on the other) has been positively checked in all cases. Therefore, the quantity $\alpha_{1/2} M_1 v$ is represented in the following. The corresponding results for hydrogen (equal to those of deuterium and muonium) and helium (equal to that of He_3) are given in Fig. 3.

In addition, we find that the angular spread follows a simple dependence with the square root of the target thickness, $c\sqrt{x}$, as illustrated by the lines in the figure (note also
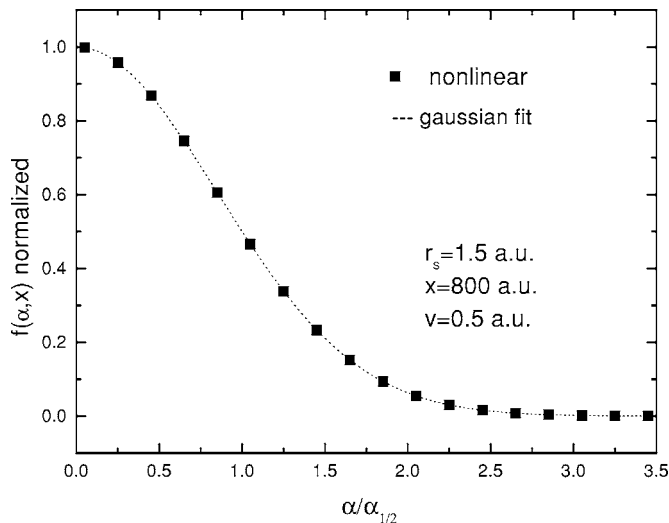
FIG. 2. Nonlinear results for the multiple-scattering function, $f(\alpha,x)$, of Eq. (22), for a FEG characterized by $r_s=1.5$. The values of α have been normalized to the half-width $\alpha_{1/2}$. The line shows a fit to the numerical results using a Gaussian function.

that this dependence is statistically consistent with the Gaussian dependence shown in Fig. 2). We should point out, however, that some deviations from this dependence have been obtained for very small thicknesses (where small deviations from the Gaussian limit were consistently observed).

The only remaining dependence on the relevant physical parameters which has not been analyzed yet, is the dependence on the electron gas density. To determine this dependence we have performed a large set of calculations for each
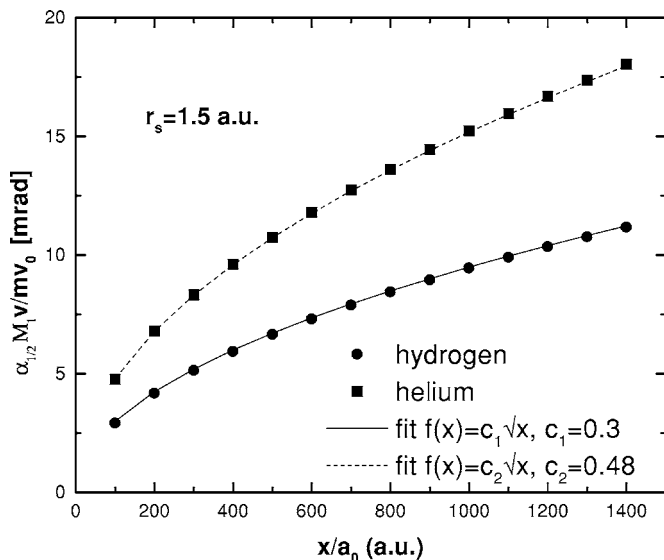

FIG. 3. Scaling of the half-width of the multiple-scattering function and its dependence with target thickness x for hydrogen and helium (and related isotopes). The results are shown in the form $\alpha_{1/2}M_1v$ related to m_pv_0, where m_p is the proton mass and v_0 is the Bohr velocity. The calculations (solid symbols) were made using the nonlinear formulation, for $v=0.5$ a.u. and $r_s=1.5$. The fitting curves are of the form $c_i\sqrt{x}$ with appropriate coefficients c_i, as indicated.
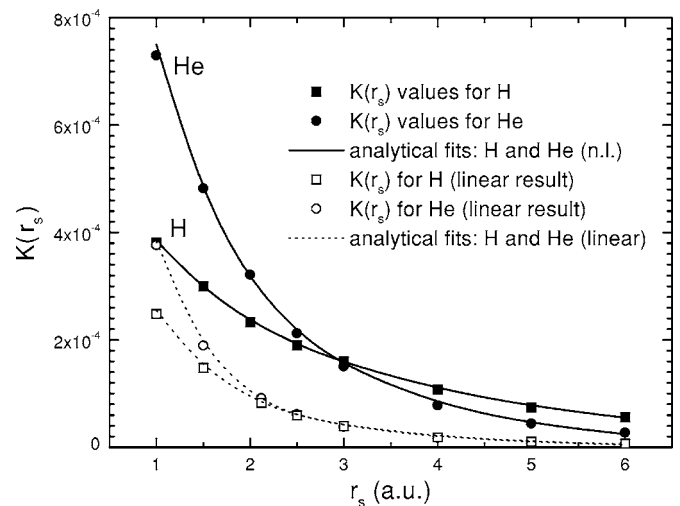

FIG. 4. Theoretical values of the coefficients $K(r_s)$, Eq. (26), for hydrogen and helium, calculated with the linear (lower curves) and nonlinear formulations (upper curves), for a wide range of r_s values ($1<r_s<6$ a.u.). The values of $K(r_s)$ were numerically determined from calculations of the half angle $\alpha_{1/2}$, for the different projectiles and associated isotopes, according to the procedure indicated in the text. The lines show the corresponding fitting curves.

of the projectiles through the range of densities of interest for valence electrons in solids, corresponding to r_s values in the range $1<r_s<6$ a.u.

The final results of the whole set of calculations may be summarized by the following analytical approximations for the half angle:

$$\alpha_{1/2} = K(r_s)\frac{m_p}{M_1}\frac{v_0}{v}\sqrt{\frac{x}{a_0}}, \qquad (26)$$

where M_1 is the ion mass and v its velocity, m_p is the proton mass, x is the target thickness, and v_0 and a_0 are the Bohr velocity and radius, respectively. The dependence on the electron gas density is contained in the coefficient $K(r_s)$ which has been numerically determined for the projectiles included in this study. The results for $K(r_s)$ obtained from the nonlinear calculations are shown in Fig. 4. The lines in the figure show the analytical fitting expressions given below.

An interesting feature that we may note in Fig. 4 is the crossing of the $K(r_s)$ lines for H and He at $r_s \cong 3$. This may be considered a replica of the similar crossing previously observed in the stopping coefficients obtained from the same nonlinear approach [23]. However, because of the isotopic effect given by the factor m_p/M_1 in Eq. (26) (which is not present in the energy loss) the electronic multiple scattering is significantly lower for He than for H in the whole range of r_s values.

As a final question, we have determined analytical fitting functions for $K(r_s)$ which could be of interest for practical purposes. The following fitting expressions yield very accurate (better than 5%) approximations to the nonlinear results through the range of r_s values explored in these calculations

$$K(r_s)_H = \frac{5.1 \times 10^{-4}}{r_s^{0.31}} \exp(-0.28 r_s), \quad (27)$$

$$K(r_s)_{He} = \frac{1.2 \times 10^{-3}}{r_s^{0.6}} \exp(-0.47 r_s). \quad (28)$$

These expressions correspond to hydrogen atoms and helium, respectively (the same results apply to the isotopes of these elements) and are shown by the continuous lines in Fig. 4.

A. Some illustrative examples

To illustrate the magnitude of the EMS effects in real cases we consider a few examples of interest.

(1) Protons with an energy of 9 keV ($v = 0.6$ a.u.) moving in a FEG with $r_s = 1.5$ (a value which is appropriate for gold targets) assuming a thickness $x = 800$ a.u.. In this case the $\alpha_{1/2}|_{FEG}$ due to electronic interactions becomes 0.8°. This may be compared with the $\alpha_{1/2}$ value for protons in gold, for the same conditions, obtained from the standard MS theory for *atomic* interaction (using Sigmund-Winterbon's approach [8]): $\alpha_{1/2}|_{atomic} \cong 37°$. It is also useful to compare these values with Lindhard's *channeling angle* [13,9] for the same case: $\psi_{1/2}|_{channeling} \cong 5.2°$.

(2) 4 keV muons in a FEG with $r_s = 1.5$ and with thickness $x = 200$ a.u.. In this case we get $\alpha_{1/2}|_{FEG} = 1.8°$, while, for the same conditions we get the corresponding values: $\alpha_{1/2}|_{atomic} \cong 31°$ and $\psi_{1/2}|_{channeling} \cong 6.3°$.

From these examples we conclude that in the case of proton beams the contribution of electronic interactions to the multiple scattering may be considered negligible for the case of random trajectories, and of relative interest for channeling conditions. On the other hand, in the case of slow muons ($m_\mu/m_p = 0.113$) or pions ($m_\pi/m_p = 0.149$) the effect becomes also small for random trajectories, but it may produce sizable effects in some channeling studies.

B. Comparison with Bonderup's estimation

As a final question, we compare the present nonlinear results with the upper limit estimate predicted by Bonderup [14]. The transport cross section in Eq. (2) may be calculated in the nonlinear approach, for a free-electron gas, using the quantal expression

$$\sigma_{tr} = \frac{4\pi}{v_F^2}\left(\frac{\hbar}{m}\right)^2 \sum_{l=0}^{\infty}(l+1)\sin^2(\delta_l - \delta_{l+1}). \quad (29)$$

Since the density functional values for the phase shifts are used, the results for σ_{tr} obtained here are in perfect agreement with those reported in previous works [17,18,23].

To obtain the upper limit to the $\alpha_{1/2}$ values, we use Eq. (2), considering also the relation between the half-width at half maximum $\alpha_{1/2}$ and the value of $\langle\delta\Phi^2\rangle$, viz., $\alpha_{1/2} = 0.833\sqrt{\langle\delta\Phi^2\rangle}$ (0.833 being $=\sqrt{\ln 2}$). The result may be written in the form of Eq. (26) with

$$K(r_s)_B = 0.833\sqrt{8}\frac{m}{m_p}\frac{v_F}{v_0}\sqrt{\sigma_{tr}n_e a_0}. \quad (30)$$
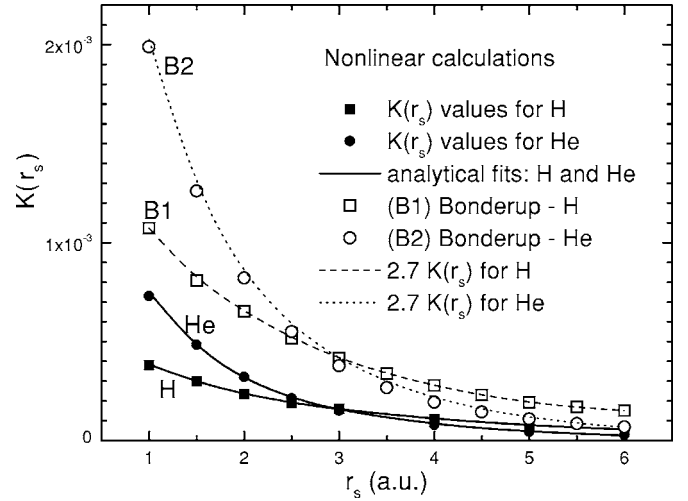

FIG. 5. Comparison between the values of $K(r_s)$ for hydrogen and helium, calculated with the nonlinear approach (solid symbols), and the upper-limit values estimated by Bonderup in terms of the transport cross section, Eqs. (2) and (30) (open symbols). The continuous lines are the fitting expressions of Eqs. (27) and (28) while the dashed and dotted lines are the results of the present calculations, for H and He, multiplied by a common factor 2.7.

In Fig. 5 we compare the values of $K(r_s)$ obtained from our calculations for hydrogen and helium (solid symbols) with the upper bond estimate of Eq. (30) (open symbols). As expected, the values from Eq. (30) are significantly larger than those of the present calculations. But it is interesting to note that the ratio between Eq. (30) and the present calculations yield nearly constant values. This means that the dependence with r_s predicted by Eq. (30) is a fairly good one. To illustrate this we have multiplied our results for H and He by a common factor 2.7 and we compare these values (dashed and dotted lines) with the prediction of Eq. (30). As it may be observed in Fig. 5 the comparison is remarkably good, and therefore the factor 2.7 yields the ratio between the upper limit estimate and the precise values obtained here.

V. SUMMARY AND CONCLUSIONS

We have investigated the influence of electronic scattering processes on the angular dispersion of light atomic projectiles moving through a free-electron gas. We developed a formulation based on the general multiple-scattering theory using the nonlinear approach to represent the interactions.

We performed a set of calculations for slow projectiles and analyzed the main features of the electronic multiple-scattering process. In particular, we find that (1) The EMS distribution, given by the function $f(\alpha,x)$, satisfies simple scaling laws with respect to the projectile mass and velocity, corresponding to angular spreads of the form $\alpha_{1/2} \sim 1/(M_1 v)$; (2) The EMS distribution is well approximated by a Gaussian function, and its half-width $\alpha_{1/2}$ increases with the square root of the target thickness, $\alpha_{1/2} \sim \sqrt{x}$. The results of this approach have been compared with a previous upper limit estimation made by Bonderup, showing now the exact magnitude of the electronic MS effects.

The results of this study are condensed in simple interpolation formulas, such as (27) and (28), representing the nonlinear results for hydrogen and helium, respectively, which yield accurate approximations to the half-width at half maximum, $\alpha_{1/2}$, in the range of r_s values of interest for solid targets. These analytical approximations may be useful in further studies using slow ion beams.

As could be expected based on physical arguments, and from the previous estimations, the magnitude of the electronic contribution to the multiple scattering of ions in real materials, in the usual situation of ions moving along random trajectories through a solid, is very small (as compared with the *atomic* multiple scattering), but they may become important in channeling experiments involving light ions or sub-

atomic particles, like muons or pions, as well as in studies related to the formation and annihilation of bound systems such as muonium or pionium. Further studies of these effects by numerical simulations would be of interest.

[1] W. Bothe, Z. Phys. **5**, 63 (1921).

[2] S. Goudsmit and J. L. Saunderson, Phys. Rev. **57**, 24 (1940); **58**, 36 (1940).

[3] G. Molière, Z. Naturforsch. A **3a**, 78 (1948).

[4] H. S. Snyder and W. T. Scott, Phys. Rev. **76**, 220 (1949).

[5] H. Bethe, Phys. Rev. **89**, 1256 (1953).

[6] W. T. Scott, Rev. Mod. Phys. **35**, 231 (1963).

[7] L. Meyer, Phys. Status Solidi B **44**, 253 (1971).

[8] P. Sigmund and K. B. Winterbon, Nucl. Instrum. Methods **119**, 541 (1974).

[9] D. S. Gemmell, Rev. Mod. Phys. **46**, 129 (1974).

[10] B. D. Patterson, Rev. Mod. Phys. **60**, 69 (1988).

[11] G. Flik, J. N. Bradbury, D. W. Cooke, R. H. Heffner, M. Leon, M. A. Paciotti, M. E. Schillaci, K. Maier, H. Rempp, J. J. Reidy, C. Boekema, and H. Daniel, Phys. Rev. Lett. **57**, 563 (1986).

[12] J. E. Valdés, P. Vargas, and N. R. Arista, Phys. Rev. Lett. **85**, 4731 (2000).

[13] J. Lindhard, K. Dan. Vidensk. Selsk. Mat. Fys. Medd. **34**, 1 (1965).

[14] E. Bonderup, *Penetration of Charged Particles through Matter*, Lecture Notes (University of Aarhus, Aarhus, 1981).

[15] J. Lindhard, K. Dan. Vidensk. Selsk. Mat. Fys. Medd. **28**, 1 (1954).

[16] R. H. Ritchie, Phys. Rev. **114**, 644 (1959).

[17] P. M. Echenique, R. M. Nieminen, and R. H. Ritchie, Solid State Commun. **37**, 779 (1981).

[18] M. J. Puska and R. M. Nieminen, Phys. Rev. B **27**, 6121 (1983).

[19] D. Pines, *Elementary Excitations in Solids* (Benjamin, New York, 1963).

[20] T. L. Ferrell and R. H. Ritchie, Phys. Rev. B **16**, 115 (1977).

[21] A. Mann and W. Brandt, Phys. Rev. B **24**, 4999 (1981).

[22] A. H. Sørensen, Nucl. Instrum. Methods Phys. Res. B **48**, 10 (1990).

[23] P. M. Echenique and M. E. Uranga, in *Interaction of Charged Particles with Solids and Surfaces*, edited by A. Gras-Martí, H. M. Urbassek, N. R. Arista, and F. Flores (Plenum, New York, 1991).

[24] M. Alducin, A. Arnau, and I. Nagy, Phys. Rev. A **68**, 014701 (2003).

[25] M. Peñalba, A. Arnau, and P. M. Echenique, Nucl. Instrum. Methods Phys. Res. B **56**, 352 (1991).

[26] A. Salin, A. Arnau, P. M. Echenique, and E. Zaremba, Phys. Rev. B **59**, 2537 (1999).

[27] I. Nagy, A. Arnau, and P. M. Echenique, Phys. Rev. B **38**, 9191 (1988).

[28] I. Nagy, A. Arnau, and P. M. Echenique, Phys. Rev. A **40**, 987 (1989).

[29] J. C. Ashley, A. Gras-Marti, and P. M. Echenique, Phys. Rev. A **34**, 2495 (1986).

[30] To extend the calculations to $r_s = 1$ (not included in the density functional calculations of Ref. [18]) we have used complementary results based on the Friedel sum rule method, as reported by A. F. Lifschitz and N. R. Arista, Phys. Rev. A **57**, 200 (1998).

[31] G. Högberg, H. Nodén, and H. G. Berry, Nucl. Instrum. Methods **90**, 283 (1970).